PHYSICAL REVIEW D **78,** 034030 (2008)

Trilepton production at the CERN LHC: Standard model sources and beyond

Zack Sullivan
Southern Methodist University, Dallas, Texas 75275-0175, USA,
and High Energy Physics Division, Argonne National Laboratory, Argonne, Illinois 60439, USA

Edmond L. Berger
High Energy Physics Division, Argonne National Laboratory, Argonne, Illinois 60439, USA
(Received 23 May 2008; published 26 August 2008)

Events with three or more isolated leptons in the final state are known to be signatures of new physics phenomena at high energy collider physics facilities. Standard model sources of isolated trilepton final states include gauge boson pair production such as WZ and $W\gamma^*$, and $t\bar{t}$ production. We demonstrate that leptons from heavy flavor decays, such as $b \to lX$ and $c \to lX$, provide sources of trileptons that can be orders of magnitude larger after cuts than other standard model backgrounds to new physics processes. We explain the physical reason heavy flavor backgrounds survive isolation cuts. We propose new cuts to control the backgrounds in the specific case of chargino plus neutralino pair production in supersymmetric models. After these cuts are imposed, we show that it should be possible to find at least a 4σ excess for supersymmetry parameter space point LM9 with 30 fb^{-1} of integrated luminosity.

DOI: 10.1103/PhysRevD.78.034030 PACS numbers: 13.85.Qk, 12.60.Jv, 13.85.Rm

I. INTRODUCTION

Events with three or more isolated leptons in the final state have attracted significant attention as possible signatures of new physics phenomena produced at high energy collider physics facilities such as the Fermilab Tevatron [1] and the CERN Large Hadron Collider (LHC) [2–6]. To the extent that new physics at the scale of 100 GeV or more is related to electroweak symmetry breaking, new states predicted in beyond the standard model (BSM) schemes typically couple to the $W^\pm$ or Z^0 gauge bosons which, in turn, decay to leptons.

Supersymmetry (SUSY) is a well studied potential realization of physics beyond the standard model [7]. Trilepton events have long been mentioned as potential golden discovery modes for SUSY processes in which a chargino $\tilde{\chi}_i^+$ and a neutralino $\tilde{\chi}_j^0$ are jointly produced. Isolated three lepton signatures arise from the decay modes $\tilde{\chi}_i^+ \to W^{*+}\tilde{\chi}_1^0 \to \bar{l}\nu\tilde{\chi}_1^0$, along with $\tilde{\chi}_j^0 \to Z^*\tilde{\chi}_1^0 \to l\bar{l}\tilde{\chi}_1^0$. In this example, the $\tilde{\chi}_1^0$ is the lowest mass SUSY particle assumed to be effectively stable and therefore a source of missing energy; W^{*+} and Z^* stand for on-shell or virtual gauge bosons. This SUSY example provides a relatively clean source of isolated trilepton events [8,9]. Within SUSY, one can also pair-produce heavy sparticles that carry the color quantum number, such as gluinos and squarks. The cascade decays of these states, while parameter dependent, will generally result in trilepton final states along with hadronic jets [10].

Other BSM constructs, such as Higgsless models, extra-dimensional models, and models with extended gauge groups, predict states at high mass, such as Kaluza-Klein towers and extra gauge bosons, that decay to the more familiar W and Z electroweak gauge bosons. In one example of a Higgsless model, a massive W' is predicted with dominant decays into pairs of gauge bosons, such as $W^\pm Z$, which is a source of isolated three lepton final states [11–13]. Our intent here is not to present a survey of BSM sources of multilepton events. We cite the cases mentioned as indicative of a range of possibilities.

In this paper we are concerned with obtaining as good an estimate as possible of the production of isolated three lepton final states that arise entirely from sources within the standard model (SM) itself. An obvious and important example is the associated production of a pair of gauge bosons, such as WZ, along with its generalizations $W\gamma^*$, where γ^* is a virtual photon that decays as $\gamma^* \to l\bar{l}$. While the importance of the $W\gamma^*$ process has been emphasized as an important background before [9,14], we demonstrate that its contribution significantly changes the expectations of the particular CMS and ATLAS studies we examine. Unlike WZ, the $W\gamma^*$ contribution cannot be reduced by an antiselection of events in which the invariant mass of the $l\bar{l}$ system is in the vicinity of the Z^0 peak.

In this work, we use MADEVENT [15] to compute the full matrix elements for partonic subprocesses that result in a $lll\nu$ final state. For the WZ/γ^* process, this method allows us to retain important angular correlations among the final leptons. Here Z/γ^* stands for the full range of $l\bar{l}$ pairs resulting from a Z, a Drell-Yan virtual photon, and photon-Z interference. Our estimates are larger for this process than those one would obtain from a modeling of WZ alone from within PYTHIA [16], and we describe these differences. Inclusion of the γ^* contribution accounts for part of these differences. Since WZ/γ^* is an important standard model background in many searches for new physics, we suggest that events be generated by a matrix element program and be fed into the PYTHIA showering

routines, rather than use of the WZ routine built into PYTHIA.

A major new contribution in this paper is the demonstration that isolated leptons from bottom and charm decays are a potent source of standard model backgrounds to new physics signatures in the three lepton final state. This study is an extension of our prior investigation [17] of SM heavy flavor backgrounds to the isolated two-lepton final state that is important in searches for the Higgs boson. In this new paper we compute contributions from a wide range of SM heavy flavor processes including bZ/γ^*, cZ/γ^*, $b\bar{b}Z/\gamma^*$, $c\bar{c}Z/\gamma^*$. We also include contributions from $t\bar{t}$ production, and from processes in which a W is produced in association with one or more heavy flavors such as tW, $b\bar{b}W$, $c\bar{c}W$. In all these cases, one or more of the final observed isolated leptons comes from a heavy flavor decay. The $b\bar{b}W$ and $c\bar{c}W$ contributions have not been examined previously.

To examine signal discrimination (and to compute signal to background ratios), we choose the specific case of chargino and neutralino pair production as the signal process. We focus on the SUSY parameter space points LM1, LM7, and LM9 considered by the CMS Collaboration [2,3] and on the SU2 point studied by the ATLAS Collaboration [5]. These points are expected to have favorable SUSY cross sections at the LHC. The dominant nature of some of the SM backgrounds motivates the investigation of new selections (cuts) on the final-state kinematic distributions that would be effective in reducing the backgrounds. One of these cuts involves selections on the opening angles among the three charged leptons in the final state. The cuts are defined and their effectiveness is discussed in Secs. IV and V.

We begin in Sec. II with an explanation of the source and magnitude of isolated leptons from heavy flavor production and decay. Issues important in our simulation of final states are discussed in Sec. III. We generate events using MADEVENT, pass them through a PYTHIA showering Monte Carlo code, and finally through a heavily modified PGS detector simulation program. Our overall results and comparisons with studies done by the CMS and ATLAS groups are presented in Secs. IV and V. Our conclusions are summarized in Sec. VI. We show that it should be possible to find at least a 4σ excess in 30 fb^{-1} for SUSY point LM9.

II. ISOLATED LEPTONS FROM BOTTOM AND CHARM DECAYS

The use of leptons inside jets to tag bottom and charm jets has led to the recognition that strong isolation criteria are required to distinguish leptons from primary interactions from those caused by secondary decays. In Ref. [17] we demonstrate that the rate for secondary leptons to pass isolation cuts is surprisingly large—about 1 part in 200. In this section we explain the reasons these leptons pass the isolation cuts at such a large rate.

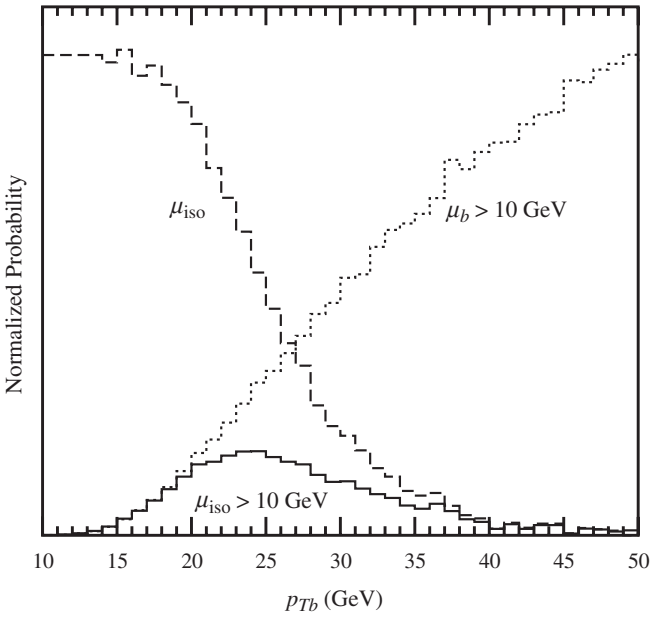

FIG. 1. Normalized probability for an existing b quark to produce an isolated muon with $p_{T\mu} > 10$ GeV (solid) vs the b transverse momentum. This curve is a multiplicative combination of the probability of producing a muon with $p_{T\mu} > 10$ GeV (dotted) and the probability the muon will be isolated (dashed). The b production spectrum is not included. Muon isolation criteria are described in the Appendix.

The simplest case to understand is the production of muons from b quark decay. The branching fraction of various B hadrons (B_d, B_s, Λ_b, etc.) to muons is roughly 9%–14%. Observation of these leptons requires, however, that their charged tracks generally be above some transverse momentum threshold (see the Appendix for details of isolated lepton reconstruction). In the dotted line of Fig. 1 we show the shape of the probability to produce a muon with $p_{T\mu} > 10$ GeV versus the transverse momentum of an initial b quark. This curve is determined predominantly from the $V - A$ matrix element decay of the B hadron into $Dl\nu$ [16] and kinematics imposed by the muon momentum threshold.[1] The probability of producing a 10 GeV muon is small at low b transverse momentum, and it grows toward the branching fraction limit as the transverse energy of the b moves farther above threshold. This curve leads to the false impression that low-p_T b quarks are unimportant.

There are two ways in which a muon can pass isolation cuts applied to detector data. The first is if the other decay

[1]There is a small dependence in the shape due to the default choice of Peterson fragmentation for $b \to B$. A slightly harder B spectrum is predicted by a nonperturbative fragmentation function [18], which in turn predicts that the leading edge of the dotted line in Fig. 1 would shift 1–2 GeV lower. This implies softer b quarks can produce 10 GeV muons, and hence would slightly *increase* the backgrounds compared to those calculated here.

products of the B hadron are physically separated in pseudorapidity η and/or radial angle ϕ. This separation accounts for no more than $1/2$ of the isolated rate. One could imagine rejecting secondary muons by increasing the area examined for accompanying radiation, but this technique reduces acceptance of primary muons and is of limited utility. Of more importance is the isolation energy cut. When muons come from low-p_T b quarks, they must have taken most of the transverse momentum of the B hadron. This means there is not enough energy left in the other B decay products to fail the energy cuts for isolation. The net isolated muon probability is the multiplication of the probability for production and for passing isolation cuts. This probability is shown as the solid line of Fig. 1, and it peaks fairly close to threshold.

There is little freedom to change the picture in Fig. 1. An attempt could be made to lower the energy threshold beyond which events are rejected, but this cut is already nearly optimized for the acceptance of real muons. Hence, one might expect to reduce the rate of muons from higher-p_T b decays, but there will not be much gain. One other handle might be to look for secondary vertices, but our tests indicate that virtually all muons that pass isolation point back at the primary vertex. A preliminary examination of CDF data [19] appears to confirm this finding.

The physics behind finding an isolated electron from b quark decay is similar to that for finding a muon. Figure 2 demonstrates the same probability for production of an electron. The probability of satisfying the isolation cuts is flatter with respect to p_{Tb} than for the muon, because noise in the electromagnetic calorimeter requires less stringent cuts to maintain electron acceptance. It is possible to achieve some purity with a loss of acceptance, but we find little difference in the net rate of leptons from heavy flavors between the ATLAS reconstruction algorithm that we use [20] and less sophisticated algorithms.

While physical limitations of the experimental apparatus control the acceptance of a lepton produced from a b decay, the overall rate of reconstructed leptons includes the effect of the p_{Tb} production spectrum. With the exception of top-quark decay, the p_{Tb} spectrum tends to fall steeply. In Fig. 3 we display the net isolated lepton cross section as a function of p_{Tb} for $b\bar{b}$ production. Despite the larger acceptance for isolated muons around $p_{Tb} \sim 25$ GeV and isolated electrons with $p_{Tb} \sim 30$–50 GeV, the peak production comes from b quarks around 20 GeV. The position of this peak has a profound effect on the simulation of isolated leptons, because fully $1/2$ of the reconstructed muon rate comes from b quarks with $p_{Tb} < 20$ GeV. A natural tendency is to ignore these lower energy b quarks based on the low probability of lepton production shown in the dotted lines of Figs. 1 and 2. The complete picture, however, demonstrates that these events are important and most difficult to reject. The net effect is that about 1% of b quarks produce a lepton (μ or e) that passes isolation cuts. This agrees with a D0 study using their full detector simulation that found ~0.5% of b hadrons produced isolated muons [21].

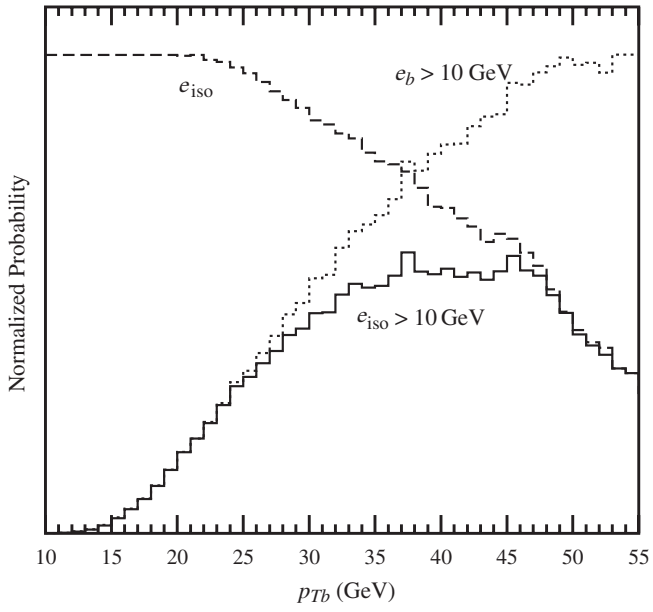

FIG. 2. Normalized probability for an existing b quark to produce an isolated electron with $p_{Te} > 10$ GeV (solid) vs the b transverse momentum. This curve is a multiplicative combination of the probability of producing an electron with $p_{Te} > 10$ GeV (dotted) and the probability the electron will be isolated (dashed). The b production spectrum is not included. Electron isolation criteria are described in the Appendix.

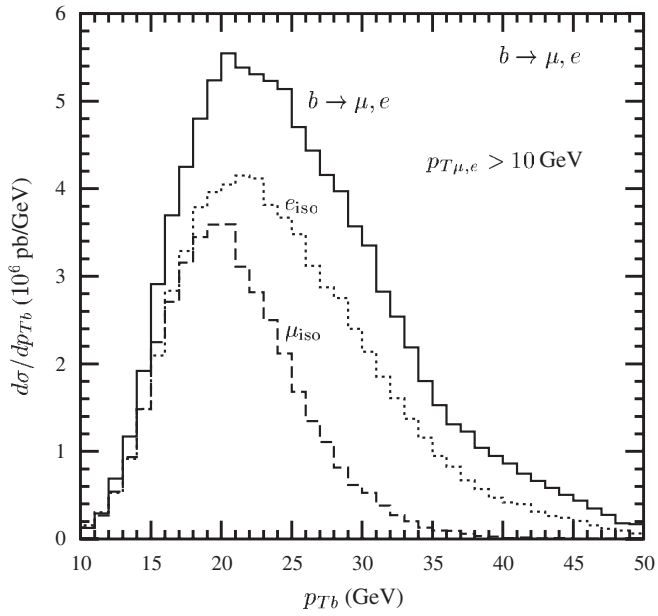

FIG. 3. Cross section for production of a muon or electron from $b\bar{b}$ production and decay (solid), an isolated muon (dashed), or an isolated electron (dotted).

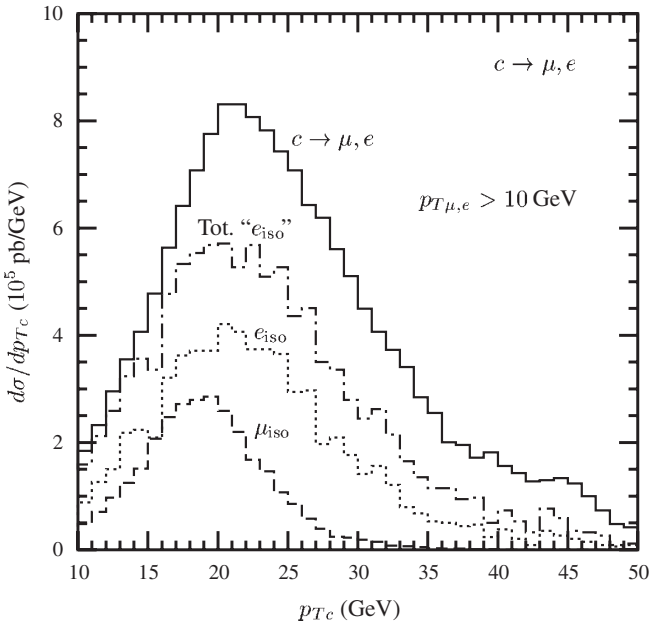

FIG. 4. Cross section for production of a muon or electron from $c\bar{c}$ production and decay (solid), an isolated muon (dashed), an electron which is then isolated (dotted), or "isolated electron" including fakes (dash-dotted).

An examination of charm decay into isolated muons and electrons leads to essentially identical conclusions as bottom decay with one minor addition. In Fig. 4 we show the cross section for production of a muon or electron vs p_{Tc}, and their isolated rates. In practice, because of "fakes" (charged hadrons mistaken for electrons), the reconstructed rate for electrons is larger than expected from the decay of c to e times an isolation acceptance. A large number of charged pions can be produced in decays of D mesons. A reasonable fraction of these pions are reconstructed as electrons, and so the net rate for "isolated electrons" shown as the dot-dashed line is about 50% larger than expected. Electron reconstruction algorithms are constructed in order to balance this contamination of charged pions versus acceptance. The goal across detectors is typically a fake rate for pions from jets of 10^{-4} (compared to the rate of leptons we find of a few times 10^{-3} from b and c decays) [20,22]. Depending of the physics study, it may be worth including the decays from heavy quarks as a part of the design of electron isolation algorithms. For the case of trileptons we examine here, the leptons from heavy quarks dominate the backgrounds.

We conclude this section by noting that Figs. 3 and 4 indicate the expected rate of isolated electrons from processes containing b and c quarks can be significantly larger than the rate for isolated muons. Consequently, new physics processes with muons should have a higher purity than those with electrons. One general strategy would be to look for signals with an excess that is more apparent in muon channels than electron channels. A second observation is that looser cuts cause the typical transverse momentum of surviving isolated electrons to be slightly higher than that for muons. This recognition suggests that electron events will be more suppressed than muon events by cuts on maximum lepton energy, e.g., the Z-peak cut used below. This lepton flavor dependence may allow an additional handle on *in situ* calibration of background sources.

III. SIMULATION

The backgrounds we discuss tend to arise from the tails or end points of physical processes and challenge detector capabilities. To achieve a believable and detailed simulation of reconstructed events, we follow the methods developed and validated in Ref. [17], with some modifications for efficient production and analysis of the results.

We generate events with a customized[2] version of MADEVENT 3.0 [15] and run them through the PYTHIA 6.327 [16] showering Monte Carlo. Both programs use the CTEQ6L1 parton distribution functions [23] evaluated via an efficient evolution code [24]. The showered events are fed through a version of the PGS 3.2 [25] fast detector simulation, modified to match ATLAS geometries, efficiencies, and detailed reconstruction procedures [20]. We confirm that our results agree with full ATLAS detector simulations at both the reconstructed object (leptons, jets, $\not{E}_T$) and analysis levels to better than 10% (and in some cases better than 1%).

For this paper we use the ATLAS muon and electron reconstruction procedure (described in the Appendix) and detector efficiencies to produce initial candidate leptons for both CMS and ATLAS studies. We then apply the CMS or ATLAS geometric acceptance, transverse momentum threshold, and analysis cuts in order to compare to their respective studies. We reproduce the results of the published CMS analysis to better than 1% in most cases. As we expect from Sec. II, and as observed in Ref. [17], we find that, since the detectors have been optimized for the same lepton acceptance and lepton fake rate from jets, the lepton rate from heavy flavor decays is insensitive to details of the detector reconstruction.

In Sec. II we explain the physics reasons for simulating low-p_T b and c quarks. In Ref. [17] we determined that at least 1000 samples of phase space are required to reproduce the interesting angular correlations in phase space for these types of events. As missing energy plays an important role in these signals, we cannot just multiply the spectrum of produced quarks by an average lepton isolation acceptance. Instead, we iterate over each point in phase space between 10^4 and 5×10^5 times, ensuring we produce at least 10 events that pass a minimal set of cuts. This number is sufficient if there are two b or c quarks that are needed to produce leptons.

[2]We use a new "zooming" procedure that improves phase space filling.

Simulating any cross section that requires 3 or more heavy quarks to produce leptons ($bbbb$, $cccc$, $bbcc$) would require at least 1000 times the number of events we simulate. Hence, we can provide only an order-of-magnitude estimate of the effect of these four heavy flavor processes in Sec. IV.

Several technical hurdles have to be overcome to achieve the statistically significant and systematically controlled results shown in Secs. IV and V. We have already described our method of iterating multiple times over the same phase-space points to give showering an opportunity to generate isolated leptons. Even though the detector simulation is technically a ''fast'' detector simulation, over 10 billion events were required to produce sufficient statistics to describe the heavy flavor decays to isolated leptons throughout their available phase space. This computation was carried out with 2 CPU years of time on the Argonne Laboratory Computing Resource Center JAZZ cluster, a Pentium Xeon Linux cluster with 350 compute nodes. The large number of events raises a practical issue regarding the total amount of data generated. Because of the time involved in generation, and our desire to analyze both angular correlations and different cuts for CMS and ATLAS, we must store event information. Standard PYTHIA, STDHEP, or compressed data structures for this analysis would require more than 100 terabytes of storage, a simply impractical requirement. Therefore, we write only events that produce at least 3 isolated leptons (see the Appendix for the definition of isolation), and store the four-vectors of the leptons, leading jet (for vetoes), and missing transverse energy. This is the minimal necessary information to analyze the data presented below.

IV. COMPARISON TO CMS

In their technical design report (TDR) [2], the CMS Collaboration defines several sets of minimal supergravity (mSUGRA) parameters that have sensitivity to different aspects of SUSY. The points LM1, LM7, and LM9 are the only subset of the nine points examined that exhibit a large trilepton signature from $\tilde{\chi}_2^0\tilde{\chi}_1^\pm$ decay. These points assume $A_0 = 0$, $\mu > 0$, and (m_0, $m_{1/2}$, $\tan\beta$) are (60, 250, 10), (3000, 230, 10), and (1450, 175, 50) for LM1, LM7, and LM9, respectively. The reach for discovery of $\tilde{\chi}_2^0\tilde{\chi}_1^\pm$ decays to trileptons is summarized in the TDR, but we follow the more detailed account from Ref. [3] below.

The basic CMS analysis looks for three isolated leptons, with $p_{T\mu} > 10$ GeV, $p_{Te} > 17$ GeV, and $|\eta_l| < 2.4$ (see the Appendix for the method of isolation). Events that contain jets with $E_{Tj} > 30$ GeV are vetoed in order to reduce the contribution from processes such as $t\bar{t}$ production and more complex SUSY processes involving cascade decays of massive SUSY states. Since real Z decays dominate the usual standard model backgrounds, events are removed in which the invariant mass of the opposite-sign same-flavor (OSSF) leptons is more than 75 GeV. CMS then performs a neural net analysis with seven variables to suppress the backgrounds from SM production of Z + jets and virtual photon + jets (called Drell-Yan in their terminology) to achieve a signal to background ratio S/B of $1/3$. There are not enough details or referenced notes regarding the neural net for us to reproduce the results, but we can confirm agreement for the backgrounds considered. However, the new backgrounds calculated here far outweigh the ones studied by CMS. As all of our estimated backgrounds are larger than those determined by CMS, we explain in detail where our simulations agree and where and why they differ.

There are three overriding observations to keep in mind. First, each significant background involving leptons from heavy flavor decays, not estimated by CMS, is more than 10 times larger than the largest background considered by CMS. Second, as explained below, our first benchmark process, WZ includes additional physics that enhances this background. Third, the ISASUGRA 7.69 evolution code used by CMS for the supersymmetric spectrum gives mass differences and branching fractions incompatible with the more recent version employed in our work. Nevertheless, we find good agreement with the CMS results when we consider only their backgrounds and use their assumptions. Therefore, we are confident that the simulation improvements discussed below are valid and will be useful for future studies.

A. WZ, $t\bar{t}$, and Wt final states

In order to maintain consistency across processes considered, we elect to present results using leading-order cross sections rather than introducing next-to-leading-

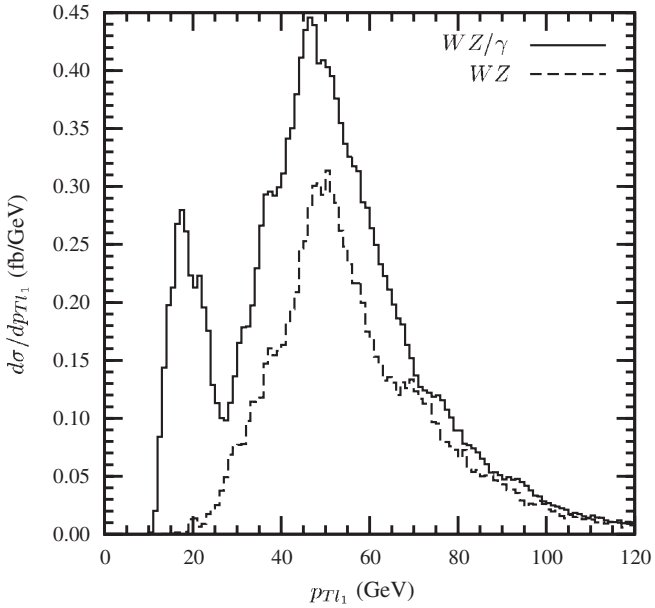

FIG. 5. Transverse momentum (p_T) distribution of the leading-p_T lepton in WZ/γ compared with WZ.

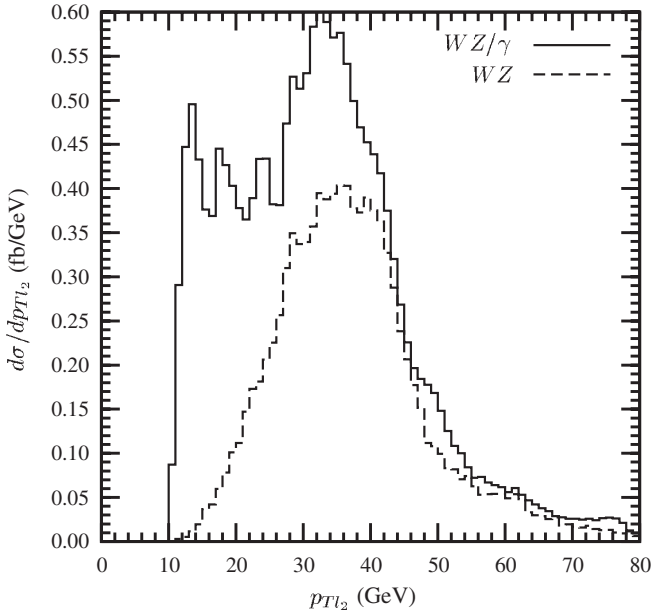

FIG. 6. Transverse momentum (p_T) distribution of the second leading-p_T lepton in WZ/γ compared with WZ.

order (NLO) K factors. While NLO calculations exist for most of these processes [26], there is considerable overlap at NLO between final states, e.g., bZ and $b\bar{b}Z$. Furthermore, the jet veto will reject some of the higher order radiation that enhances the cross sections. Proper matching between orders is beyond the scope of this paper.

Since our goal is to establish a direct connection with the CMS analysis, we first confirm that our detector simulation reproduces the CMS detector simulation for reconstructed leptons. Performing a PYTHIA-based calculation of WZ, minus decays to taus, and using the CMS K-factor of 2, we predict 171 events after cuts in 30 fb^{-1} vs 173 events in Table 6 of the CMS analysis [3]. Any differences in lepton reconstruction enter 3 times; hence, this comparison shows that our detector simulation agrees exceedingly well with the CMS detector simulation.

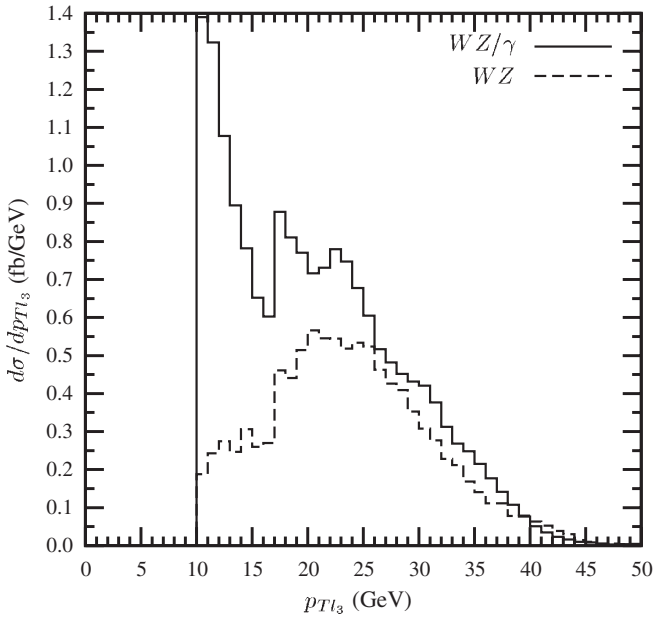

FIG. 7. Transverse momentum (p_T) distribution of the lowest-p_T lepton in WZ/γ compared with WZ.

The PYTHIA code used by CMS for WZ production omits virtual photon γ^* production and interference with the Z. Given that the Z peak will be removed by cuts, we find that the additional contribution from W plus a virtual photon is at least as important. This result agrees with other work [9,14] in which the importance of the virtual photons is emphasized. In all of our simulations, we include the virtual photon continuum and photon-Z interference along with the Z. In the case of the SM WZ contribution, we denote the full contribution from WZ, $W\gamma^*$, and $W + Z$, γ^* interference by WZ/γ. In Figs. 5–7 we show the transverse momentum distribution of the p_T-ordered leptons from WZ/γ compared with the distributions from WZ alone. The peak at 20 GeV in Fig. 5 is produced by the minimum p_T cuts on the individual leptons that make up the virtual photon contribution. Essentially all of the leptons from off-shell photons survive the Z-peak mass cut. When there are 3 muons or 3 electrons, both OSSF pairings pass the cuts. Hence, about $1/2$ of the virtual photon events appear twice when counting events.

Table I compares the LO WZ/γ cross section with a virtual photon included to a CMS-like NLO WZ estimate using PYTHIA. Given that a K-factor of 2 is used in the CMS estimate, there is a full factor of 6 difference between WZ built into PYTHIA, and WZ/γ generated by MADEVENT and showered by PYTHIA. Nearly $1/2$ of the excess is attributable to the virtual photon that is not included in PYTHIA. Some of the excess comes from correlations captured by the full matrix element that are sensitive to the cuts. In particular, angular correlations among the final-state leptons are missing from the CMS study. In order to study

TABLE I. Comparison of two backgrounds calculated by CMS and by this study. WZ/γ and $t\bar{t}$ are our estimates. WZ_{PYT} is calculated from PYTHIA and normalized to the CMS NLO total cross section. $t\bar{t}_{\mathrm{CMS}j}$ uses the CMS acceptance for the jet veto, based on a matched calculation that produces significantly more radiation than a leading-order calculation. The second column shows the number of events expected with 30 fb^{-1} of integrated luminosity after the requirements that there be three leptons and no jets with $E_{Tj} > 30$ GeV. In the third column an additional requirement is imposed that the invariant mass of any pair of OSSF leptons be no greater than 75 GeV.

Channel	$N^l = 3$, No jets	$M_{ll}^{\mathrm{OSSF}} < 75$ GeV
WZ/γ^{LO}	1880	538
$t\bar{t}$	1540	814
$WZ_{\mathrm{PYT}}^{\mathrm{NLO}}$	661	171
$t\bar{t}_{\mathrm{CMS}j}$	394	208

these correlations, and to quote a more realistic background, we use the full matrix element for $WZ/\gamma \to lll\nu$ from MADEVENT showered through PYTHIA in our results below.

The remaining increase in the normalization of the cross section is connected with the requirement that there be no jets with $E_T > 30$ GeV. We compare $WZ \to lll\nu$ events generated with MADEVENT and showered with PYTHIA to WZ events which are generated, decayed, and showered all within PYTHIA. In the process we observe that the initial-state QCD radiation spectrum is harder in the all-PYTHIA events. The jet veto rejects a larger fraction of this pure electroweak process assuming PYTHIA generation, and hence leads to a smaller normalization of the cross section after cuts. This effect is consistent across all processes we calculate, and hence leads to an overall uncertainty in the absolute cross section. Our main concern in this paper is to understand the *relative* importance of the various backgrounds, and their shapes. When data are in hand, we expect the total background to be normalized to data. Because most of the processes we evaluate are not in PYTHIA, we perform and demonstrate the cross sections for MADEVENT generated events, and discuss the effect of normalization on a discovery signal at the end.

CMS also quotes their estimated background from $t\bar{t}$ production. It is important to compare with their result because this background requires one lepton from a b decay. The CMS analysis uses a matched [27] $t\bar{t}$ cross section which produces more jets in the final state than our LO calculation. Hence, CMS has a higher rejection rate based on their jet veto. If we rescale our result using the efficiency of their jet veto instead of ours, we find 208 events in 30 fb^{-1} vs 239 events in the CMS paper. We find excellent agreement between our estimate of a background with a lepton from a b and the CMS estimate. A similar rescaling for Wt would give us 37 events vs 45 in the CMS paper. Our systematic 10% underestimate of the effect of isolated leptons from b decay in the $t\bar{t}$ sample suggests our other results involving leptons from heavy flavor decays are conservative. The comparison between our calculation of $t\bar{t}$ and the jet-acceptance reduced version are summarized in Table I.

B. Heavy flavor final states

Before addressing the importance of leptons from heavy flavor decays, we comment on one subtlety in the supersymmetric models studied. The 243 events we find for SUSY point LM9 are similar to the 238 events expected by CMS. However, we predict 123 events vs 91 for point LM7, and 44 events vs 70 events for LM1. The differences are attributable to the use of ISASUGRA 7.75 in our study vs ISASUGRA 7.69 by CMS.[3] There was a small bug in the evolution codes in ISASUGRA 7.69 that, when corrected, leads to 10 GeV shifts in the neutralino mass spectrum. The Z mass-peak cut is sensitive to the end point of the lepton spectrum, $M_{ll}^{\max} = \sqrt{(m_{\tilde{\chi}_2^0}^2 - m_{\tilde{l}}^2)(m_{\tilde{l}}^2 - m_{\tilde{\chi}_1^0}^2)/m_{\tilde{l}}^2}$ for the three-body decays at LM1, and $M_{ll}^{\max} = m_{\tilde{\chi}_2^0} - m_{\tilde{\chi}_1^0}$ for LM7 and LM9. The end point for LM1 is just above the Z mass-peak cut, and the results are sensitive to small shifts in the neutralino masses. Additionally, branching fractions for LM7 change between ISASUGRA versions as τ's are predicted to become more or less important. Therefore, only point LM9 is directly comparable to the CMS study we discuss here, but we include the other points as future studies will likely use the newer evolution formulas.

TABLE II. Leading-order signal and background statistics for several final states in a CMS-like analysis, and with two additional cuts. The second column shows the number of events expected with 30 fb^{-1} of integrated luminosity after the requirements that there be three isolated leptons and no jets with $E_{Tj} > 30$ GeV. In the third column an additional requirement is imposed that the invariant mass of any pair of OSSF leptons be no greater than 75 GeV. The virtual photon components are large after cuts.

Channel	$N^l = 3$ No jets	$M_{ll}^{\rm OSSF} < 75$ GeV	$\not{E}_T > 30$ GeV	Angular Cuts
LM9	248	243	160	150
LM7	126	123	89	85
LM1	46	44	33	32
WZ/γ	1880	538	325	302
$t\bar{t}$	1540	814	696	672
tW	273	146	123	121
$t\bar{b}$	1.1	1.0	0.77	0.73
bZ/γ	14000	6870	270	177
cZ/γ	3450	1400	45	35
$b\bar{b}Z/\gamma$	8990	2220	119	103
$c\bar{c}Z/\gamma$	4680	1830	69	35
$b\bar{b}W$	9.1	7.6	5.6	5.3
$c\bar{c}W$	0.19	0.15	0.12	0.11

In the previous subsection, we establish agreement in three cases in which we can compare directly with CMS. In this subsection, we turn to our main results. In Table II we show the number of signal and background events expected with 30 fb^{-1} in our CMS-like analysis. For each subprocess we list the number of trilepton events expected after the jet veto is applied as well as the number of events that survive the Z peak mass cut. We also tabulate the number of events that survive after two additional cuts which we describe below.

Addressing the contributions of Z/γ plus heavy flavors and W plus heavy flavors, we see in Table II that, before the Z peak cut, Z/γ plus heavy flavors produces trileptons 16 times more often than WZ/γ. After the Z peak cut, the ratio rises to 23 times WZ/γ. In particular, $b\bar{b}Z/\gamma$, which includes a virtual photon, is over 30 times the CMS esti-

[3]We are unable to use ISASUGRA 7.69 due to a change in data format.

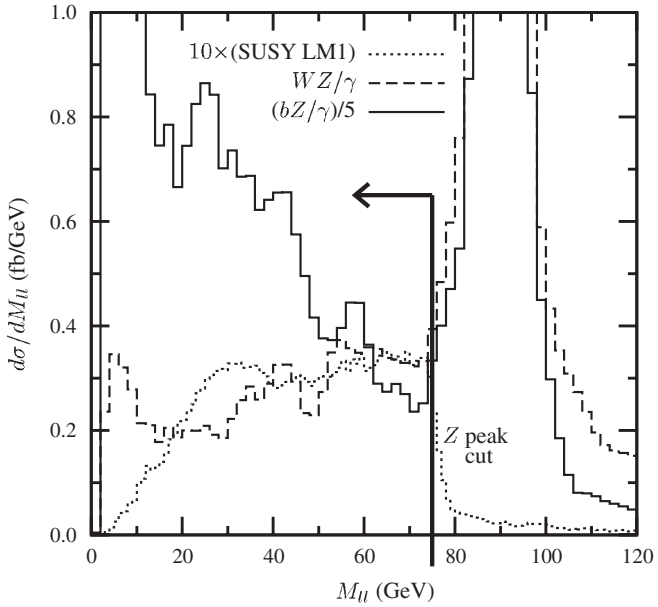

FIG. 8. Invariant mass of the opposite-sign same-flavor (OSSF) lepton pairs for the SUSY LM1 signal ($\times$ 10, dotted), the WZ/γ background (dashed), and the bZ/γ background (divided by 5, solid). Other Z/γ + heavy flavor backgrounds (not shown) have the same shape as bZ/γ.

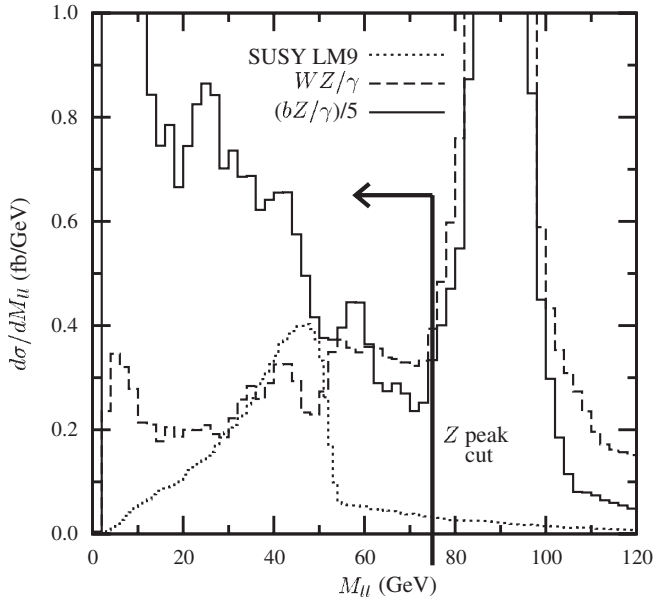

FIG. 10. Invariant mass of the opposite-sign same-flavor (OSSF) lepton pairs for the SUSY LM9 signal (dotted), the WZ/γ background (dashed), and the bZ/γ background (divided by 5, solid). Other Z/γ + heavy flavor backgrounds (not shown) have the same shape as bZ/γ.

mate of the cross section that does not have a photon. In Figs. 8–10, we see the opposite-sign same-flavor (OSSF) dilepton invariant mass for the signals, WZ/γ background, and $(bZ/\gamma)/5$. Cutting out the Z mass peak reduces the backgrounds, but the remaining tail for Z/γ plus heavy flavors overwhelms the signal.

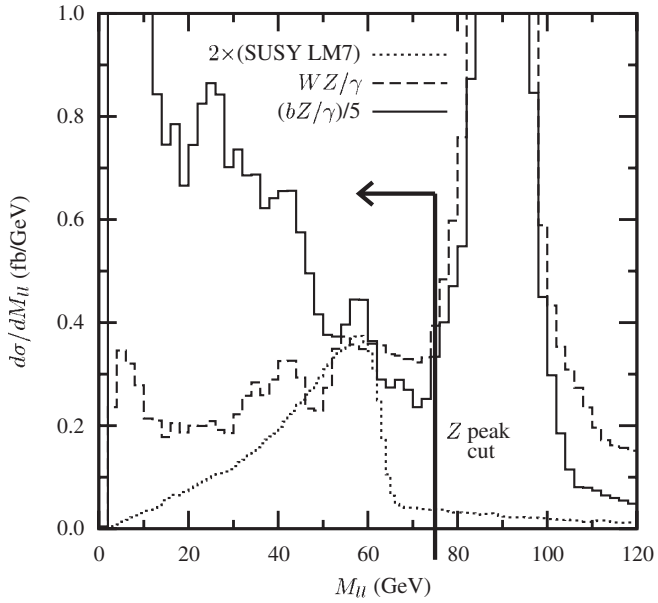

FIG. 9. Invariant mass of the opposite-sign same-flavor (OSSF) lepton pairs for the SUSY LM7 signal ($\times$ 2, dotted), the WZ/γ background (dashed), and the bZ/γ background (divided by 5, solid). Other Z/γ + heavy flavor backgrounds (not shown) have the same shape as bZ/γ.

The number of handles available to reject the huge background from Z/γ + heavy flavors is limited. In Ref. [17] we recommend raising the minimum lepton p_T threshold since the lepton p_T spectrum from b and c decays tends to fall rapidly. In typical trilepton studies, however, the leptons are very soft. Hence, any increase in the cut on the lepton p_T tends to reject too much of the signal.

Missing transverse energy $\not{E}_T$ is a partial discriminator. The SUSY signals contain invisible neutralinos which leave a broad range of $\not{E}_T$ in the detector. In Fig. 11 we show the $\not{E}_T$ spectrum for the SUSY LM9 signal and for the WZ/γ and bZ/γ backgrounds. Trilepton signatures from $t\bar{t}$ production generally have two neutrinos which lead to large missing energy. The contribution from Z/γ + heavy flavor processes peaks at over 400 times the size of the LM9 signal at low $\not{E}_T$, but it falls rapidly to below the signal by $\not{E}_T > 50$ GeV. These differences present both opportunities and challenges, especially since the precision of $\not{E}_T$ measurements is not as great as one might prefer.

In the fourth column of Table II, we show that the requirement $\not{E}_T > 30$ GeV removes most of the Z/γ + heavy flavor backgrounds[4] for a modest loss of signal. A cut below 20 GeV is not as useful and is likely not achiev-

[4]We do not estimate the Z/γ + light jets background here because it requires an accurate prediction of the rate for jets to fake leptons. However, Z/γ + light jets has a nearly identical $\not{E}_T$ spectrum. Hence, a $\not{E}_T$ cut should perform similarly well.

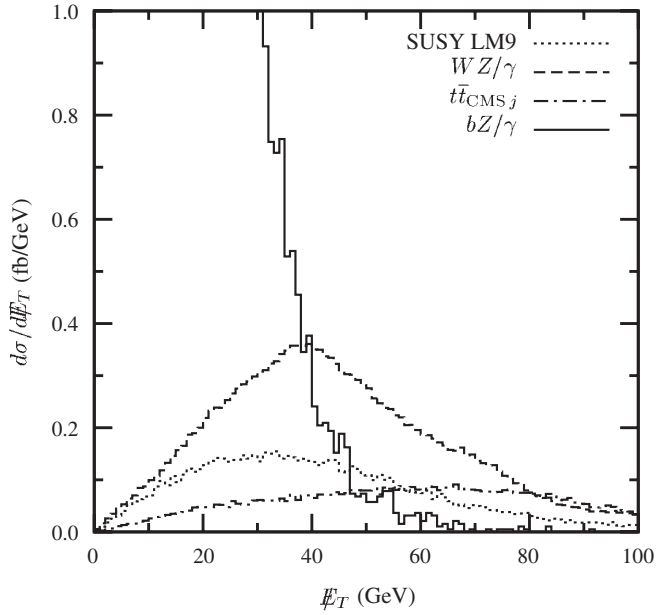

FIG. 11. Missing transverse energy spectrum $\not{E}_T$ of the opposite-sign same-flavor (OSSF) lepton pairs for the SUSY LM9 signal (dotted), the WZ/γ background (dashed), $t\bar{t}$ (dot-dashed), and bZ/γ (solid). Other Z + heavy flavor backgrounds (not shown) have the same shape as bZ/γ.

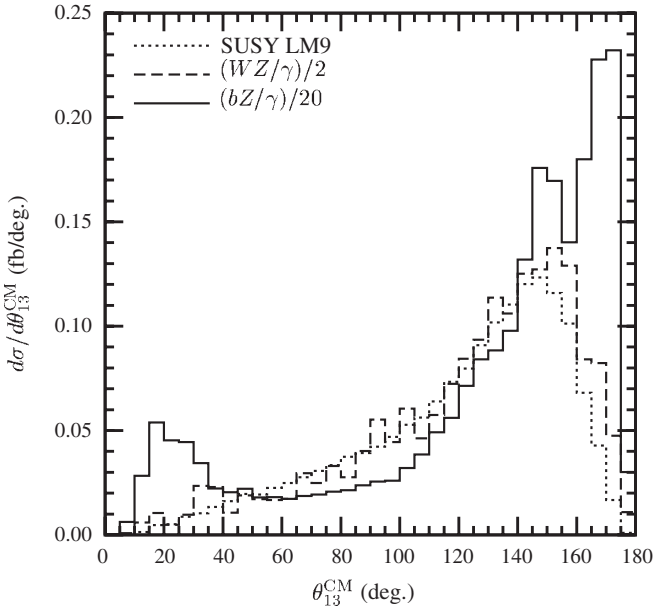

FIG. 13. Angular distribution between the leading and third p_T-ordered lepton in the trilepton center-of-momentum frame. $t\bar{t}$ is nearly identical in shape to SUSY LM9, and the $Z/\gamma + X$ backgrounds are similar to bZ/γ.

able at the LHC. A cut above 40 GeV removes most of the $Z/\gamma + X$ backgrounds, but it begins to significantly reduce the signal and is of little additional help with WZ/γ and $t\bar{t}$ backgrounds. The sharply falling $\not{E}_T$ spectrum in $Z/\gamma + X$ is extremely sensitive to uncertainties in the measurement of $\not{E}_T$. This uncertainty makes it difficult to predict absolute cross sections after cuts. On the other hand, this sensitivity could provide an excellent opportunity to *measure the background in situ* and reduce concerns regarding modeling details. The background can be fit in the data and the $\not{E}_T$ cut adjusted to optimize the purity of the sample.

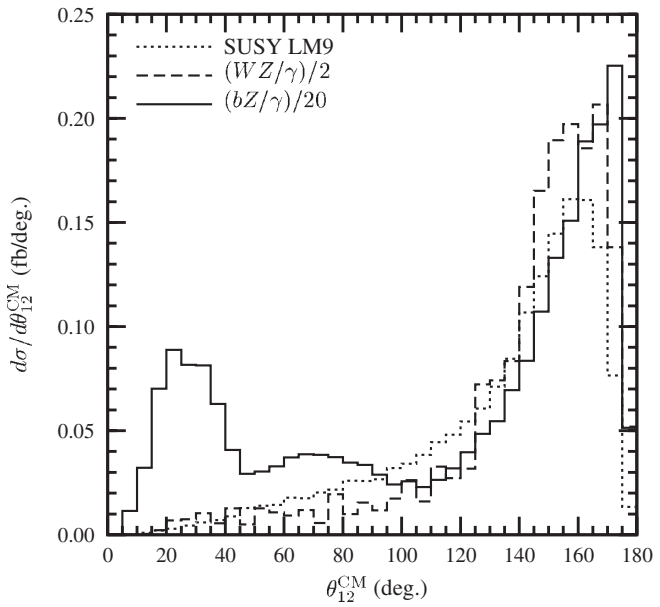

FIG. 12. Angular distribution between the leading p_T-ordered leptons in the trilepton center-of-momentum frame. $t\bar{t}$ is nearly identical in shape to SUSY LM9, and the $Z/\gamma + X$ backgrounds are similar to bZ/γ.

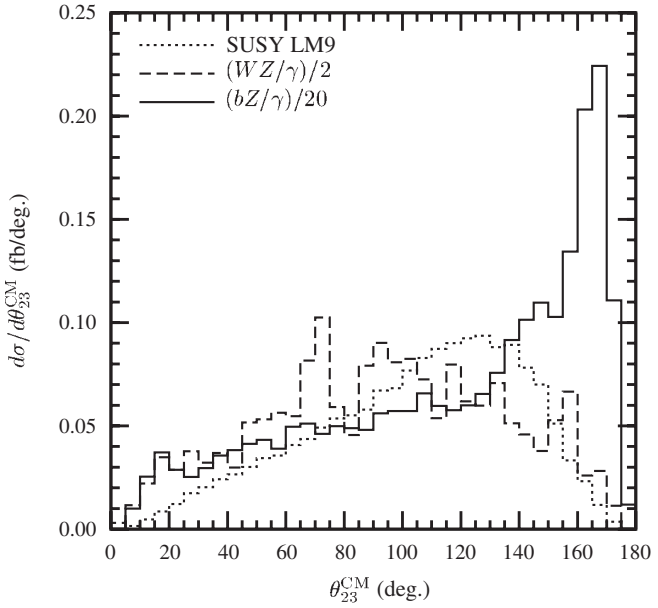

FIG. 14. Angular distribution between the second and third p_T-ordered lepton in the trilepton center-of-momentum frame. $t\bar{t}$ is nearly identical in shape to SUSY LM9, and the $Z/\gamma + X$ backgrounds are similar to bZ/γ.

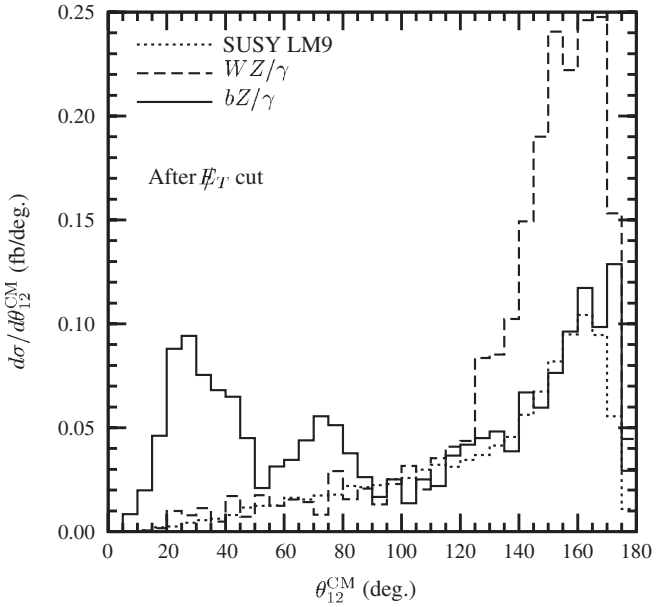

FIG. 15. Angular distribution between the leading p_T-ordered leptons in the trilepton center-of-momentum frame, after a missing energy cut $\not{E}_T > 30$ GeV. $t\bar{t}$ is nearly identical in shape to SUSY LM9, and the $Z/\gamma + X$ backgrounds are similar to bZ/γ.

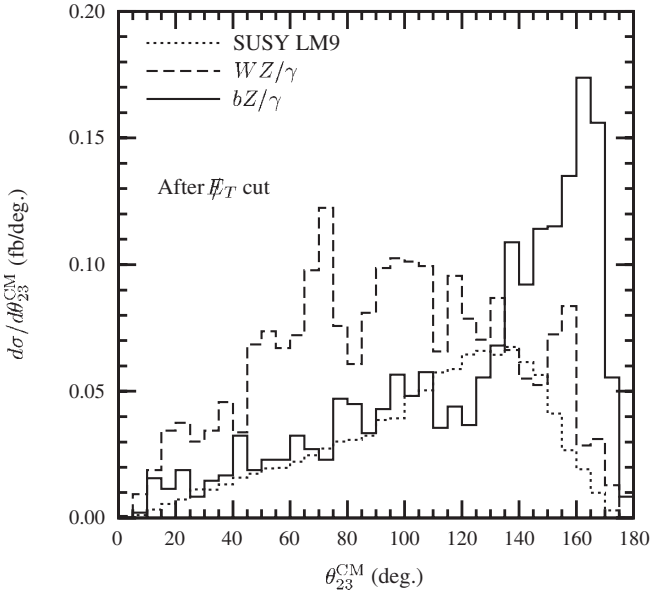

FIG. 17. Angular distribution between the second and third p_T-ordered lepton in the trilepton center-of-momentum frame, after a missing energy cut $\not{E}_T > 30$ GeV. $t\bar{t}$ is nearly identical in shape to SUSY LM9, and the $Z/\gamma + X$ backgrounds are similar to bZ/γ.

Since the accuracy of $\not{E}_T$ measurements is limited, we examine instead the utility of angular cuts without a $\not{E}_T$ cut. There are significant angular correlations in the $Z/\gamma +$ heavy flavor backgrounds that are different from those in the SUSY trilepton signals or the WZ/γ and $t\bar{t}$ backgrounds. In Figs. 12–14 we plot the angular distribution $\theta_{ij}^{\rm CM}$ between pairs of p_T-ordered leptons in the trilepton center-of-momentum (CM) frame without a $\not{E}_T$ cut. The $Z/\gamma +$ heavy flavor backgrounds have significant peaks at both small and large angles. The signal and other backgrounds either peak only at large angles ($\theta_{12}^{\rm CM}$, $\theta_{13}^{\rm CM}$), or are fairly central ($\theta_{23}^{\rm CM}$).

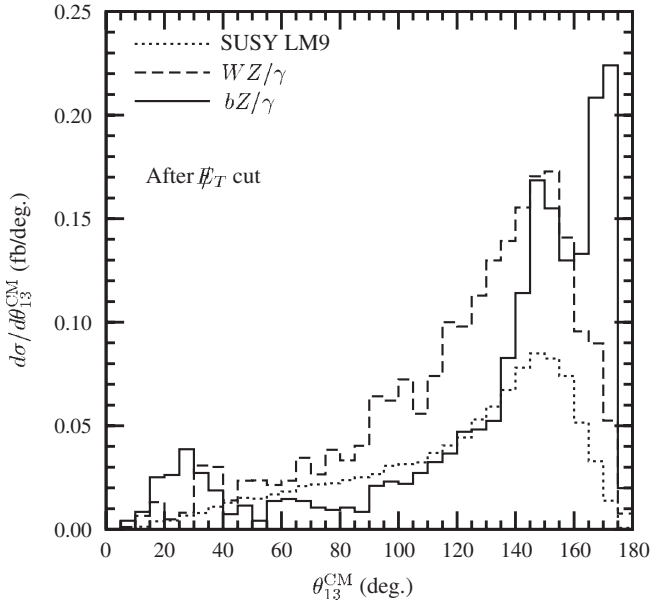

FIG. 16. Angular distribution between the leading and third p_T-ordered lepton in the trilepton center-of-momentum frame, after a missing energy cut $\not{E}_T > 30$ GeV. $t\bar{t}$ is nearly identical in shape to SUSY LM9, and the $Z/\gamma + X$ backgrounds are similar to bZ/γ.

We examine the impact of these angular correlations by themselves by imposing three angular cuts in the trilepton center-of-momentum frame: $\theta_{12}^{\rm CM} > 45°$, $\theta_{13}^{\rm CM} > 40°$, and $\theta_{23}^{\rm CM} < 160°$. These angle cuts reduce the heavy flavor backgrounds and WZ/γ by $\sim$30%, with only a 5% reduction of the signal. These cuts could be further optimized, but in general they are more useful for increasing purity than for increasing significance.

Figures 15–17 show the angular distributions between pairs of p_T-ordered leptons in the trilepton CM frame after the missing transverse energy cut. The last column of Table II demonstrates the effect of adding the three angular cuts after the $\not{E}_T$ cut. There is almost no correlation between the effects of the angle cuts and the missing transverse energy cut except in bZ/γ, where the cut is slightly more effective after the $\not{E}_T$ cut (acceptance is 0.32 vs 0.37). The real advantage of angular cuts over a $\not{E}_T$ cut is that the angles are well measured. Whether or not missing transverse energy can be well measured, the use of the angular cuts will improve any final analysis.

One class of backgrounds not treated so far is one in which all three leptons come from heavy flavor production

($b\bar{b}b\bar{b}$, $c\bar{c}c\bar{c}$, $b\bar{b}c\bar{c}$). As mentioned in Sec. III, practical limitations prevent us from simulating this background directly. Instead we provide rough estimates for the trilepton signature from three sources of $b\bar{b}b\bar{b}$ production. First, using $Wb\bar{b}$ production, we obtain an estimate for the probability of finding an isolated lepton at the LHC of 7.5×10^{-3} per b. The cross section for direct production of $b\bar{b}b\bar{b}$ from MADEVENT multiplied by $(7.5 \times 10^{-3})^3$ gives about 500 trilepton events in 30 fb^{-1} of data. Second, multiple interactions per beam crossing, where more than one $b\bar{b}$ pair is produced, can lead to a trilepton signature. For a total inelastic cross section of about 80 mb [2], the rate for two scatters to give three isolated leptons is about 60 events per interaction per 30 fb^{-1}.[5] At 10 interactions per crossing, this method leads to about 600 events, though the jet veto will likely reduce this figure somewhat.

Multiple scattering in a given interaction (e.g., double parton scattering), or even showering of heavy quarks, is a third source, arising from successive production of $b\bar{b}$ pairs. The rate may be comparable to direct 4-b production after cuts on transverse momentum [28], and it can double the backgrounds listed so far. These rough estimates are the same order of magnitude as the number of events from Z/γ + heavy flavor processes, and they are a potentially serious problem with the default analysis. A sum over all production processes and decays to both muons and electrons would increase these numbers by an order of magnitude. On the other hand, in Ref. [17] we observe that a missing energy cut serves to significantly reduce the net cross section from pure QCD processes. Even if the suppression is only as strong as for Z/γ + heavy flavors, the background can and should be measured *in situ* as a function of $\not{E}_T$, and then removed by adjusting the $\not{E}_T$ cut as needed.

Unlike the CMS study in Ref. [3], we find that the $E_T >$ 30 GeV jet veto and the Z mass-peak cut are not sufficient to find more than a 2σ evidence for SUSY point LM9 (the most optimistic). However, the addition of a cut on $\not{E}_T$ is sufficient to find at least a 4σ excess (and perhaps an 8σ excess if a CMS-like initial-state radiation estimate is used). In Table III, we summarize our expected sensitivity in 30 fb^{-1} for point LM9. We also estimate the sensitivity after the background from fakes is included (using fake rates from Table 6 of the CMS study). The background from fakes has little effect on the final analyses. The angular cuts mentioned above do not appear to influence the significance of the signal, but we emphasize again that angles will be much better measured than missing transverse energy and may be useful in compensating for experimental uncertainties. The other SUSY points studied do less well with any cuts. Using the more optimistic CMS-like jet veto scenario and Tables II and III, we find the best significance for points LM7 and LM1 to be 4.2σ and 1.6σ, respectively, in 30 fb^{-1} of integrated luminosity.

TABLE III. The significance for SUSY point LM9 is listed for each cut, as well as the significance assuming all background events are reduced to the CMS jet veto acceptance (a reduction factor of 3.6). In parentheses are estimates of the total significance assuming additional detector backgrounds from Table 6 of the CMS analysis not directly evaluated in this study.

	$N^l = 3$ No jets	$M_{ll}^{\mathrm{OSSF}} < 75$ GeV	$\not{E}_T > 30$ GeV	Angular Cuts
$S/\sqrt{B}_{\mathrm{LM9}}$	1.33	2.07(1.79)	3.93(3.74)	3.94(3.79)
$S/\sqrt{B}_{\mathrm{LM9}}^{\mathrm{CMS}\,j}$	2.63	4.09(3.54)	7.78(7.39)	7.79(7.49)

We conclude this section with a note regarding flavor and sign combinations. For the SUSY trilepton signals and standard model backgrounds we consider, there is no difference in production rate of the states $\mu\mu\mu$, $e\mu\mu$, $ee\mu$, or eee. Any observed difference is expected to come from the slightly larger acceptance for isolated electrons over muons from heavy-quark decays, balanced against the slightly larger rejection of electron events over muons from the Z-peak mass cut. This fact may be useful as a check of detector acceptances, but it has no power to resolve the signal. The $W^{\pm}Z/\gamma$, $tW^{\pm}$, $b\bar{b}W^{\pm}$, and $c\bar{c}W^{\pm}$ cross sections will produce a slight enhancement of two positive leptons over two negative leptons since parton distribution functions for protons favor W^+ production over W^- production (e.g., W^+Z/γ: $W^-Z/\gamma \approx 3{:}2$). It may be possible to use this sign difference to constrain the total $W + X$ background in this sample *in situ*, and improve the control of some systematic errors. Overall, this type of analysis may be useful for discovery of BSM trilepton signatures that favor the production of muons over electrons (or vice versa).

V. COMPARISON TO ATLAS

The ATLAS Collaboration has considered the search for supersymmetry in the trilepton channel for a long time [4]. More recently, the ATLAS Collaboration has been utilizing trilepton signatures from supersymmetry to study variations on electron identification and jet rejection algorithms. We examine trileptons in the context of the SU2 test point as examined in preliminary contributions to the ATLAS CSC 7 Note [5]. The SU2 test point is in the "focus point" region of mSUGRA parameter space, and its parameters are $m_0 = 3550$ GeV, $m_{1/2} = 300$ GeV, $A_0 = 0$ GeV, $\tan\beta = 10$, and $\mu > 0$.

One subtlety is that the SUSY evolution in ISASUGRA 7.75 predicts that, if the top-quark mass is less than 175 GeV, these mSUGRA parameters fail to break electroweak symmetry. The lightest neutralino mass is extremely sensitive to the top-quark mass here, e.g., $m_{\tilde{\chi}_1^0}$ changes by 20 GeV with a 100 MeV shift in the top-quark mass. Hence, we tune the top-quark mass to 175.1 GeV in

[5]Multiply the ratio of $b\bar{b}$ production to total inelastic cross section times the $b\bar{b}$ cross section.

order to reproduce the mass spectrum used by ATLAS as closely as possible. Ultimately the specific model is not important, but rather we desire an estimate of how small a cross section can be observed in the general analysis given the standard model backgrounds.

The basic ATLAS analysis [5] is nearly identical to that used by CMS, with a few modifications we indicate here. They first demand three isolated leptons (see the Appendix), where $p_{T\mu} > 10$ GeV and $p_{Te} > 15$ GeV, and they veto events with jets having $E_{Tj} > 20$ GeV. The default analysis then invokes a maximum separation cut between OSSF leptons of $\Delta R_{ll} < 2.6$, to emphasize the region of phase space in which the signal is most significant. The Z peak is removed by cutting out the OSSF invariant mass region 80 GeV $< M_{ll}^{\mathrm{OSSF}} <$ 100 GeV; and a modest amount of missing transverse energy is required $\not{E}_T > 10$ GeV.

We begin by comparing how well we reproduce the ATLAS expectations for the signal. For the SU2 fixed point, ATLAS considers the simultaneous production of $\tilde{\chi}_i^0 \tilde{\chi}_j^{\pm}$, where $i = 2$–4, and $j = 1, 2$. For this analysis we examine only $\tilde{\chi}_2^0 \tilde{\chi}_1^+$, as was done for CMS. For 30 fb^{-1} of integrated luminosity, the ATLAS study expects 37 events after cuts from $\tilde{\chi}_2^0 \tilde{\chi}_1^{\pm}$ alone. We obtain excellent agreement with 37 events after cuts once we scale up the production cross section by 1.28 to match the input cross section used by ATLAS. Rather than list results scaled to older analyses, we present our results below using the newer ISASUGRA 7.75 spectrum.

Our acceptance for WZ agrees well at each cut level with the PYTHIA-based ATLAS analysis we are following. However, the missing virtual photon contribution to trileptons from $W\gamma^*$ is again important to the total number of background events. Our estimate of 466 events from $t\bar{t}$ agrees well the 453 events expected by the ATLAS study. This adds confirmation that we reproduce ATLAS expectations for leptons, jets, and $\not{E}_T$ even after cuts.

In Table IV we summarize our results for the ATLAS-like study of the SU2 focus point. At the level of three leptons and no jets, and after the default ATLAS cuts, the trilepton signature from heavy flavor decays plus a Z or virtual photon exceeds the other standard model backgrounds by at least a factor of 10. The weak missing transverse energy cut $\not{E}_T > 10$ GeV is not sufficient to effectively reduce the background from Z/γ + heavy flavor decays. Raising the cut on missing transverse energy to $\not{E}_T > 30$ GeV does reduce the background of trileptons from heavy flavors by a factor of 10, but bZ/γ is still 10 times the SU2 signal. Adding the same angular cuts we suggest in Sec. IV B, $\theta_{12}^{\mathrm{CM}} > 45°$, $\theta_{13}^{\mathrm{CM}} > 40°$, and $\theta_{23}^{\mathrm{CM}} < 160°$ reduces the background of leptons from heavy flavor decays by 30% with little effect on the signal.

The SU2 fixed point region of supersymmetry studied by ATLAS is unlikely to produce a measurable trilepton signature. Summing over both $\tilde{\chi}_2^0 \tilde{\chi}_1^+$ and $\tilde{\chi}_3^0 \tilde{\chi}_1^+$ production could require 450 fb^{-1} of data for a 5σ discovery. Nevertheless, other regions of SUSY parameter space, such as those in the CMS study we examine, are viable and share the same backgrounds we present here. Our intent is to demonstrate that, even under the differently optimized cuts applied by the ATLAS study, the backgrounds to trileptons from heavy flavors completely dominate the sample unless additional cuts are made that explicitly target their removal. A missing transverse energy cut that balances the loss of SUSY trilepton signal against background removal, and cuts based on angular correlations, are both effective means of controlling the background of leptons from heavy flavor decays.

TABLE IV. Leading-order signal and background statistics for 30 fb^{-1} in an ATLAS-like analysis, and with two additional cuts. The virtual photon components are large after cuts. For point SU2 we simulate only $\tilde{\chi}_2^0 \tilde{\chi}_1^+$ production. ATLAS considers $\tilde{\chi}_3^0 \tilde{\chi}_1^+$ production as well, which would roughly double the SUSY cross section.

	$N^l = 3$			Angular
Channel	No jets	$M_{ll}^{\mathrm{OSSF}} < 75$ GeV	$\not{E}_T > 30$ GeV	Cuts
SU2	38	29	22	21
WZ/γ	1450	387	292	272
$t\bar{t}$	942	466	409	396
tW	225	116	100	98
$t\bar{b}$	0.95	0.73	0.60	0.56
bZ/γ	12700	3200	226	138
cZ/γ	3080	571	36	26
$b\bar{b}Z/\gamma$	7760	882	88	75
$c\bar{c}Z/\gamma$	4110	745	53	38
$b\bar{b}W$	8.2	5.9	4.6	4.3
$c\bar{c}W$	0.16	0.12	0.09	0.08

VI. CONCLUSIONS

In this paper we investigate standard model sources of isolated three lepton final states at LHC energies. We provide quantitative estimates of the rates and kinematic distributions in phase space of events that arise from several processes. One of these is the associated production of WZ, along with its generalizations $W\gamma^*$, where γ^* is a virtual photon that decays as $\gamma^* \to l\bar{l}$. A major new contribution is the demonstration that bottom and charm meson decays produce isolated three lepton events that can overwhelm the effects of other processes. We compute contributions from a wide range of SM heavy flavor processes including bZ/γ^*, cZ/γ^*, $b\bar{b}Z/\gamma^*$, $c\bar{c}Z/\gamma^*$. We also include contributions from $t\bar{t}$ production, and from processes in which a W is produced in association with one or more heavy flavors such as tW, $b\bar{b}W$, $c\bar{c}W$. In all these cases, one or more of the final observed isolated leptons comes from a heavy flavor decay. These heavy flavor sources dominate the isolated lepton spectrum at small p_T, and these sources of background must be considered

in the evaluation of the significance of any signal that has low-p_T leptons.

Trileptons from WZ production have been examined previously, but we find that the $W\gamma^*$ contribution is much more significant than is widely appreciated, as has also been noted by others [9,14]. Unlike WZ, the $W\gamma^*$ contribution cannot be reduced by an antiselection of events in which the invariant mass of the $l\bar{l}$ system is in the vicinity of the Z^0 peak.

The dominant behavior of the SM sources motivates the investigation of new selections (cuts) on the final-state kinematic distributions that would be effective in reducing the backgrounds. One of these cuts involves selections on the opening angles among the three charged leptons in the final state. Our studies identify specific distributions that can be examined once real data are available and used to constrain both the shape and magnitude of the standard model backgrounds. The strongest of these is the steeply falling distribution in missing transverse energy.

We use MADEVENT [15] to compute the full matrix elements for partonic subprocesses that result in a $lll\nu$ final state. This method allows us to retain important angular correlations among the final leptons. These parton level events are then passed through a PYTHIA showering Monte Carlo code, and finally through a modified PGS detector simulation program. We compare our overall results with studies done by the CMS and ATLAS groups.

To examine signal discrimination (and to compute signal to background ratios), we choose as a signal process the supersymmetry example of chargino and neutralino pair production. We focus on the SUSY parameter space points LM1, LM7, and LM9 considered by the CMS Collaboration [2,3] and on the SU2 point studied by the ATLAS Collaboration [5]. Some of these points are expected to have favorable SUSY cross sections at the LHC.

Using the new additional cuts on $\not{E}_T$ and angles that we suggest in this paper, we show that, even after the heavy flavor backgrounds are taken into account, it should be possible to find an approximately 4σ excess in 30 fb^{-1} for SUSY point LM9 and somewhat smaller significances for points LM7 and LM1. However, we acknowledge that there are limitations inherent in modeling of events and simulations of detector response. These uncertainties are difficult to evaluate quantitatively. In particular, we note that our SM model cross sections are computed at leading order and then passed through the PYTHIA showering code. Accompanying hadronic radiation is generated by PYTHIA, and jet vetoes (no jets with $E_T > 30$ GeV) are then applied in the analysis, removing some fraction of the cross section. PYTHIA currently treats events generated internally and events fed into it differently when producing initial-state radiation. The jet veto is very sensitive to the details of this radiation spectrum, and hence there is uncertainty in the overall normalization of the events we simulate. A dedicated study of these differences in PYTHIA should be performed before ATLAS and CMS attempt to fit their measurements of initial-state radiation and of underlying events. Regardless of the normalization, this showering issue has little effect on the ratio of leptonic events coming from heavy flavor decays to those from WZ/γ^* or $t\bar{t}$.

An alternative approach would begin with next-to-leading order matrix elements and a showering code that deals properly with matching and double counting aspects of the radiation. Not having this tool available, and recognizing that it also will have its limitations, we provide an alternative (and more optimistic) assessment of the signal significance based on a partially *ad hoc* approach. The CMS study finds that, as a result of the jet veto applied in the analysis, the trilepton background obtained from a next-to-leading-order computation of the $t\bar{t}$ final state is about a factor of 3.6 smaller than one would obtain from a leading-order computation. Applying this factor of 3.6 universally to all the SM backgrounds we compute, we can obtain an approximately 8σ excess in 30 fb^{-1} for SUSY point LM9. We will not know which estimate of initial-state hadronic radiation is more correct until it is measured at the LHC.

The analysis for the ATLAS focus point SU2 is similar to the CMS analysis. The spectrum of the model near SU2 is exceptionally sensitive to assumptions regarding the top-quark mass, and it produces too few events to observe. Nevertheless, the analysis is applicable across a broad range of SUSY parameters that produce trilepton signatures, and the backgrounds remain the same. By default ATLAS applies an additional modest missing transverse energy cut and angular correlation. However, the conclusion remains that the backgrounds including leptons from heavy flavor decays are still much larger than WZ/γ^* or $t\bar{t}$.

In general, we find that the dominant backgrounds to low-momentum trilepton signatures come from real b and c decays. In the CMS and ATLAS supersymmetric analyses we examine, the Z/γ^* + heavy flavor decay backgrounds are a factor of 10–30 larger than WZ/γ^* or $t\bar{t}$ to trileptons. Large $\not{E}_T$ cuts and angular correlations can be used to significantly reduce the heavy flavor backgrounds, but we must be mindful of the modest $\not{E}_T$ in the SUSY signal. Coupled with the results for dileptons in Ref. [17], it is clear that leptons from heavy flavor decays should be examined for all low-momentum lepton signals. Once normalizations are measured *in situ*, we have handles to reduce the effect of these backgrounds to an acceptable level.

ACKNOWLEDGMENTS

We thank Tim Stelzer for sharing his improved phase-space code. Z. S. is supported by the U.S. Department of Energy under Contract No. DE-FG02-04ER41299, and is a visitor at Argonne National Laboratory. E. L. B. is supported by the U.S. Department of Energy under Contract No. DE-AC02-06CH11357 and thanks the Kavli Institute

for Theoretical Physics (KITP), Santa Barbara, for hospitality during the final stages of this work. The KITP is supported by the National Science Foundation under Grant No. NSF PHY05-51164. We gratefully acknowledge the use of JAZZ, a 350-node computer cluster operated by the Mathematics and Computer Science Division at Argonne as part of the Laboratory Computing Resource Center.

APPENDIX: ISOLATED LEPTON RECONSTRUCTION

The isolation criteria for muons and electrons used in this paper are based on the ATLAS working definitions that were publicly available at the time of this study [20]. While final criteria will likely change, we explain in Sec. II and Ref. [17] why the rate of isolated leptons from b and c decay is fairly stable. We use these same criteria to define isolated leptons for the CMS study. We apply additional cuts on transverse momentum for the CMS and ATLAS studies as described in Secs. IV and V.

A muon is said to be isolated if there is a charged track with $p_{T\mu} > 10$ GeV, a hit in the muon chamber at $|\eta_\mu| < 2.5$, and two isolation cuts are passed. The sum of the transverse momentum of all other tracks in a cone of size $\Delta R = 0.2$ must be less than an isolation energy of 4 GeV, and the sum of the energies in all calorimeter towers surrounding the one containing the muon that lie within a cone of size $\Delta R = 0.4$ must be less than 10 GeV. Finally, a pseudorapidity-dependent detector efficiency is applied that averages over cracks, noise, etc., of ≈ 0.836 for $|\eta_\mu| < 1.05$, and ≈ 0.922 for $1.05 < |\eta_\mu| < 2.5$.

Electron reconstruction is based on first defining "regions of interest" (ROI). A fixed 0.1×0.1 window in η–ϕ space is scanned over electromagnetic calorimeter towers in the region $|\eta| < 2.5$ and $0 \leq \phi < 2\pi$ and used to identify ROI with $E_T^{\mathrm{EM}} > 10$ GeV and $E_T^{\mathrm{had}} < 2$ GeV. The segmentation of the ATLAS electromagnetic (EM) calorimeter leads to towers of approximately 0.05×0.05. The energy in the 12 towers surrounding the four towers of the ROI are added, and isolation requires $E_{12} < 3$ GeV. Finally, we require the ROI to have a track within a cone of 0.1 with $0.7 < E_T^{\mathrm{EM}}/p_T^{\mathrm{trk}} < 1.4$, and apply an overall efficiency of ≈ 0.723.

[1] V. M. Abazov *et al.* (D0 Collaboration), Phys. Rev. Lett. **95**, 151805 (2005); T. Aaltonen *et al.* (CDF Collaboration), Phys. Rev. D **77**, 052002 (2008).
[2] A. de Roeck *et al.* (CMS Collaboration), Technical Design Report Vol. II, CERN-LHCC-2006-021.
[3] W. de Boer *et al.*, CMS Note 2006/113.
[4] S. Muanza and G. Montarou, ATLAS Internal Note PHYS-No-99, 1997.
[5] T. Potter and A. de Santo, ATLAS SUSYCscNote7 working group meeting, May 2007 (unpublished).
[6] W. Vandelli, Ph.D. thesis, Pavia University [CERN-THESIS-2007-072].
[7] H. E. Haber and G. L. Kane, Phys. Rep. **117**, 75 (1985); J. A. Aguilar-Saavedra *et al.*, Eur. Phys. J. C **46**, 43 (2006).
[8] D. Dicus, S. Nandi, and X. Tata, Phys. Lett. **129B**, 451 (1983); A. Chamseddine, P. Nath, and R. Arnowitt, Phys. Lett. **129B**, 445 (1983); H. Baer and X. Tata, Phys. Lett. **155B**, 278 (1985); H. Baer, K. Hagiwara, and X. Tata, Phys. Rev. Lett. **57**, 294 (1986); Phys. Rev. D **35**, 1598 (1987); P. Nath and R. Arnowitt, Mod. Phys. Lett. A **2**, 331 (1987); R. Arnowitt, R. M. Barnett, P. Nath, and F. Paige, Int. J. Mod. Phys. A **2**, 1113 (1987); R. Barbieri, F. Caravaglios, M. Frigeni, and M. Mangano, Nucl. Phys. **B367**, 28 (1991); H. Baer and X. Tata, Phys. Rev. D **47**, 2739 (1993); J. Lopez, D. Nanopoulos, X. Wang, and A. Zichichi, Phys. Rev. D **48**, 2062 (1993); **52**, 142 (1995); H. Baer, C. Kao, and X. Tata, Phys. Rev. D **48**, 5175 (1993); H. Baer, C.-H. Chen, F. Paige, and X. Tata, Phys. Rev. D **50**, 4508 (1994); S. Mrenna, G. Kane, G. Kribs, and J. Wells, Phys. Rev. D **53**, 1168 (1996); K. Matchev and D. Pierce, Phys. Rev. D **60**, 075004 (1999); H. Baer, C.-H. Chen, M. Drees, F. Paige, and X. Tata, Phys. Rev. Lett. **79**, 986 (1997); Phys. Rev. D **58**, 075008 (1998); V. Barger, C. Kao, and T. Li, Phys. Lett. B **433**, 328 (1998); W. Beenakker, M. Klasen, M. Kramer, T. Plehn, M. Spira, and P. M. Zerwas, Phys. Rev. Lett. **83**, 3780 (1999); **100**, 029901(E) (2008); S. Abel *et al.* (SUGRA Working Group Collaboration), in *Physics at Run II: the Supersymmetry/Higgs Workshop, Fermilab, 1998*, edited by M. Carena and J. Lykken (Fermilab, Batavia, 2002), p. 27.
[9] H. Baer, M. Drees, F. Paige, P. Quintana, and X. Tata, Phys. Rev. D **61**, 095007 (2000); V. D. Barger and C. Kao, Phys. Rev. D **60**, 115015 (1999); K. T. Matchev and D. M. Pierce, Phys. Lett. B **467**, 225 (1999); H. Baer, T. Krupovnickas, S. Profumo, and P. Ullio, J. High Energy Phys. 10 (2005) 020.
[10] H. Baer, C.-H. Chen, F. Paige, and X. Tata, Phys. Rev. D **53**, 6241 (1996); H. Baer, X. Tata, and J. Woodside, Phys. Rev. D **41**, 906 (1990); **45**, 142 (1992); A. Djouadi, Y. Mambrini, and M. Muhlleitner, Eur. Phys. J. C **20**, 563 (2001); H. Baer, H. Prosper, and H. Summy, Phys. Rev. D **77**, 055017 (2008).
[11] H. J. He *et al.*, Phys. Rev. D **78**, 031701 (2008).
[12] For some LHC phenomenology, see G. Brooijmans *et al.*, arXiv:0802.3715.
[13] Heavy gauge bosons related to Kaluza-Klein excitations are discussed in M. S. Carena, E. Ponton, J. Santiago, and C. E. M. Wagner, Phys. Rev. D **76**, 035006 (2007), and references therein.
[14] J. M. Campbell and R. K. Ellis, Phys. Rev. D **60**, 113006 (1999).
[15] F. Maltoni and T. Stelzer, J. High Energy Phys. 02 (2003)

027.
[16] T. Sjostrand, P. Eden, C. Friberg, L. Lonnblad, G. Miu, S. Mrenna, and E. Norrbin, Comput. Phys. Commun. **135**, 238 (2001); T. Sjostrand, L. Lonnblad, S. Mrenna, and P. Skands, arXiv:hep-ph/0308153.
[17] Zack Sullivan and Edmond L. Berger, Phys. Rev. D **74**, 033008 (2006).
[18] M. Cacciari and P. Nason, Phys. Rev. Lett. **89**, 122003 (2002).
[19] Collin Wolfe (private communication).
[20] A. Airapetian *et al.* (ATLAS Collaboration), ATLAS Technical Design Report Vol. I, CERN-LHCC-99-14; with updates from B. Mellado, S. Paganis, W. Quayle, and Sau Lan Wu, Report No. ATL-CAL-2004-002 (unpublished); F. Derue and C. Serfon, ATLAS-PHYS-PUB-2005-016 (unpublished).
[21] V. M. Abazov *et al.* (D0 Collaboration), Phys. Rev. Lett. **93**, 141801 (2004).
[22] CMS Collaboration, Technical Design Report Vol. I, Report No. CERN-LHCC-2006-001.
[23] J. Pumplin, D. R. Stump, J. Huston, H. L. Lai, P. Nadolsky, and W. K. Tung, J. High Energy Phys. 07 (2002) 012.
[24] Zack Sullivan, Comput. Phys. Commun. **168**, 25 (2005).
[25] M. Carena *et al.* (Higgs Working Group Collaboration), in *Physics at Run II: the Supersymmetry/Higgs Workshop, Fermilab, 1998* (Ref. [8]), p. 424.
[26] Many next-to-leading order results can be obtained from the Monte Carlo program MCFM, cf. [14]. Other NLO publications include L. J. Dixon, Z. Kunszt, and A. Signer, Phys. Rev. D **60**, 114037 (1999) and Nucl. Phys. **B531**, 3 (1998).
[27] S. R. Slabospitsky and L. Sonnenschein, Comput. Phys. Commun. **148**, 87 (2002).
[28] A. Del Fabbro and D. Treleani, Phys. Rev. D **66**, 074012 (2002).